Video Article

Double-barreled and Concentric Microelectrodes for Measurement of Extracellular Ion Signals in Brain Tissue

Nicole Haack[1], Simone Durry[1], Karl W. Kafitz[1], Mitchell Chesler[2], Christine Rose[1]

[1]Institute of Neurobiology, Heinrich Heine University Düsseldorf

[2]Departments of Physiology and Neuroscience, New York University School of Medicine

Correspondence to: Christine Rose at rose@uni-duesseldorf.de

URL: http://www.jove.com/video/53058
DOI: doi:10.3791/53058

Keywords: Neuroscience, Issue 103, neurosciences, acute brain slice, hippocampus, extracellular space, ion-selective microelectrode, electrophysiology, sodium, potassium, glutamate

Date Published: 9/5/2015

Citation: Haack, N., Durry, S., Kafitz, K.W., Chesler, M., Rose, C. Double-barreled and Concentric Microelectrodes for Measurement of Extracellular Ion Signals in Brain Tissue. *J. Vis. Exp.* (103), e53058, doi:10.3791/53058 (2015).

Abstract

Electrical activity in the brain is accompanied by significant ion fluxes across membranes, resulting in complex changes in the extracellular concentration of all major ions. As these ion shifts bear significant functional consequences, their quantitative determination is often required to understand the function and dysfunction of neural networks under physiological and pathophysiological conditions. In the present study, we demonstrate the fabrication and calibration of double-barreled ion-selective microelectrodes, which have proven to be excellent tools for such measurements in brain tissue. Moreover, so-called “concentric” ion-selective microelectrodes are also described, which, based on their different design, offer a far better temporal resolution of fast ion changes. We then show how these electrodes can be employed in acute brain slice preparations of the mouse hippocampus. Using double-barreled, potassium-selective microelectrodes, changes in the extracellular potassium concentration ($[K^+]_o$) in response to exogenous application of glutamate receptor agonists or during epileptiform activity are demonstrated. Furthermore, we illustrate the response characteristics of sodium-sensitive, double-barreled and concentric electrodes and compare their detection of changes in the extracellular sodium concentration ($[Na^+]_o$) evoked by bath or pressure application of drugs. These measurements show that while response amplitudes are similar, the concentric sodium microelectrodes display a superior signal-to-noise ratio and response time as compared to the double-barreled design. Generally, the demonstrated procedures will be easily transferable to measurement of other ions species, including pH or calcium, and will also be applicable to other preparations.

Video Link

The video component of this article can be found at http://www.jove.com/video/53058/

Introduction

Electrical signaling in the brain is based on the flux of ions across plasma membranes. Major ion movements into and from the extracellular space are not only mediated by passage through voltage-gated ion channels, but also by postsynaptic ionotropic receptors as well as ion transporters. Neuronal activity is thus accompanied by complex changes in the extracellular concentration of all major ions [1]. For example, influx of sodium into neurons during excitatory activity has been shown to result in a decrease in the extracellular sodium concentration ($[Na^+]_o$) [2]. The same holds true for the extracellular calcium concentration because calcium ions rapidly enter both pre- and postsynaptic structures [3]. At the same time, potassium moves the opposite way and this mediates an increase in the extracellular potassium concentration ($[K^+]_o$) in the low mM range [4,5]. Synaptic activity also causes changes in extracellular pH that are partly mitigated by concomitant glial membrane fluxes that change intraglial pH [6,7]. These activity-related changes in extracellular ion concentrations have significant functional consequences. For example, even small increases in $[K^+]_o$ depolarize neurons as well as glial cells thereby altering neuronal excitability, and several mechanisms exist to remove excess potassium [8]. Failure of these may result in epileptiform activity of neurons or phenomena like spreading depression [1].

Because of their critical importance, quantitative determination of extracellular ion concentrations is often necessary and required to understand the function and dysfunction of neural networks under physiological and pathophysiological conditions. For decades, double-barreled ion-selective microelectrodes have proven to be excellent tools for such measurements in brain tissue [9]. For many ions, highly specific sensors with low cross-reactivity for other ions are available. In addition to the classical double-barreled electrodes, so-called concentric electrodes were recently introduced. The latter provide a superior time resolution, but take a little more time and effort to construct [10].

In the following, we will describe the preparation and calibration of these two types of ion-selective microelectrodes. We then show how these electrodes can be employed in brain slice preparations for measurement of changes in $[K^+]_o$ or $[Na^+]_o$ induced by excitatory activity following different stimulation paradigms including bath and pressure application of drugs.

Protocol

This study was carried out in strict accordance with the institutional guidelines of the Heinrich Heine University Düsseldorf, Germany, as well as the European Community Council Directive (86/609/EEC). All experiments were communicated to and approved by the Animal Welfare Office at the Animal Care and Use Facility of the Heinrich Heine University Düsseldorf, Germany (institutional act number: O52/05). In accordance with the German Animal Welfare Act (Tierschutzgesetz, Articles 4 and 7), no formal additional approval for the post-mortem removal of brain tissue was necessary.

1. Preparation of Double-barreled Ion-selective Microelectrodes

1. Prepare two borosilicate glass capillaries with filament: one with a length of 7.5 cm and an outer diameter of 1.5 mm to be used for the ion-sensitive barrel, and one with a length of 6.5 cm and an outer diameter of 1.0 mm for the later reference barrel.
2. Clean the capillaries in acetone for 12 hr and then rinse several times with abs. ethanol and let them dry. Electrodes can now be stored in a desiccator.
3. Use two-component glue or a small stripe of aluminum foil to fix a long and a short capillary together at both ends. Heat the double-capillary in a furnace at 60 °C for 1 hr. This accelerates the curing process. Store the electrodes now in a desiccator.
4. Center the double-capillary into a vertical puller with a revolvable chuck. Heat the coil gently until the glass is soft enough to allow a horizontal rotation of the revolvable chuck by 180°. During this step, prevent elongation of the capillary with a chock under the chuck.
5. After cooling, remove the mechanical break and apply a second heating protocol to pull out the capillary, resulting in two sharp, double-barreled capillaries (**Figure 1**). The tip diameter of one double-capillary should be close to 1 µm.

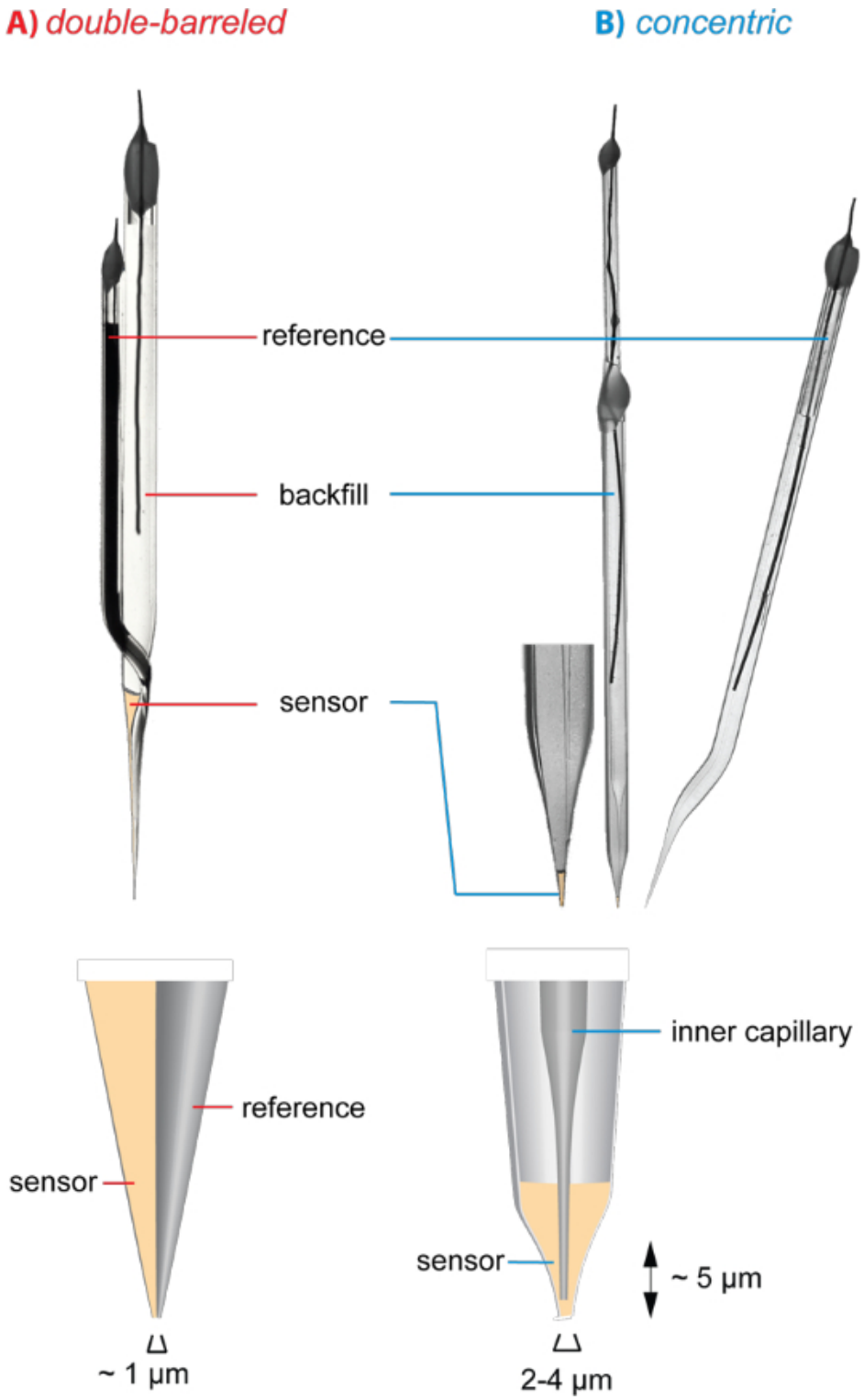

Figure 1. Architecture of ion-selective microelectrodes. (**A**) Photograph of a double-barreled microelectrode. For illustration purposes and better visibility, the liquid inside the reference barrel was tinted. (**B**) Photograph of a concentric microelectrode and the corresponding reference electrode. The tip of concentric microelectrode is shown enlarged at its left. In (**A**) and (**B**), the space occupied by the ion sensor in the tips of the pipettes is post-colored. At the bottom, the tip arrangement of both electrode types is shown schematically. Please click here to view a larger version of this figure.

6. If a vertical puller with revolvable chuck is not available, prepare a double-barrelled ion-selective microelectrode in a horizontal puller using theta glass.

1. To this end, pull theta glass (outer diameter of 1.5 mm, length 7.5 cm) out to result in two electrodes with two barrels each. Mark one of them to serve as the future reference barrel. Silanized the other similar to the procedure described below to serve as the future ion-selective barrel.
   NOTE: While the preparation of double-barreled theta-glass electrodes is far easier than the preparation of twisted double-barreled electrodes, they are more prone to cross-action between both barrels as the thin separating glass wall between them tends to be porous in their utmost tip.
   NOTE: Because the sensor cocktail (see below) is hydrophobic, the inner surface of the later ion-sensitive barrel must be rendered hydrophobic as well by a process called silanization. For this, hexamethyldisilazane (HMDS) is used (**Figure 2**) as described in the next step.

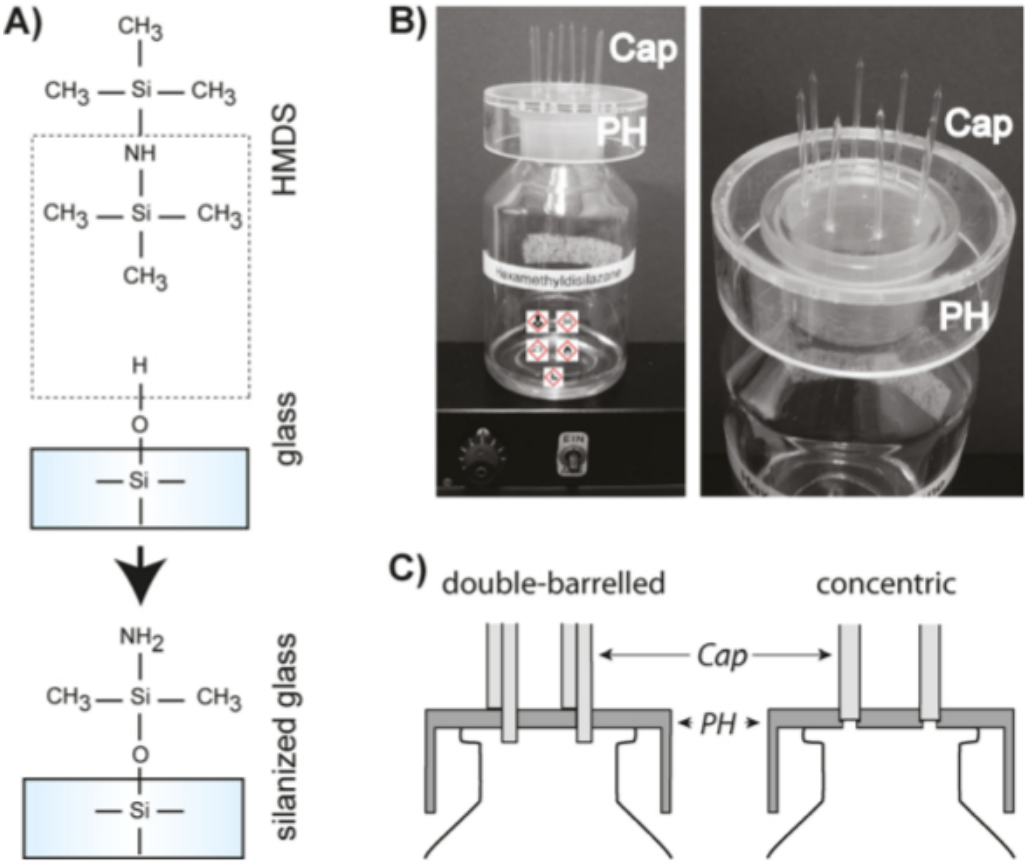

Figure 2. Silanization of pipettes. (**A**) Hexamethyldisilazane (HMDS) reacts with the Si-OH groups of the inner glass surface and renders it hydrophobic. (**B**) The left photograph shows the entire silanization unit. A wide-mouth bottle containing HMDS is placed on top of a heating plate set at 40 °C. On top of the bottle, a holder (PH) carrying the capillaries (Cap) is mounted. The right photograph shows an enlargement of the pipette holder (PH) carrying the capillaries (Cap). (**C**) Schematic side view of the custom-made pipette holders (PH) for double-barrelled (left) or concentric (right) capillaries (Cap) as mounted on a wide-mouth bottle. Please click here to view a larger version of this figure.

7. Just before pulling electrodes, fill approx. 20 ml HMDS into a wide-mouth bottle. Attention: HMDS is for use in a fume hood only, vapors are hazardous to health! Close the bottle and put it onto a heating plate, preset to 40 °C. Preheat a furnace, placed under the hood as well, up to 200 °C.
8. Fill the reference barrel up to its tip with distilled water to prevent its silanization during the following procedure.
9. Put double-barreled capillary with its tip up onto a special, custom-made holder (**Figure 2B**, **2C**). The blunt open end must reach freely through the bottom of the holder (**Figure 2C**, left). Afterwards, place this holder onto the wide mouth bottle containing the pre-warmed HMDS for 70 min.
   NOTE: Make sure that HMDS vapor can flow through capillaries freely. During one silanization process, the 20 ml of HMDS do not evaporate completely, and the bottle can thus be used multiple times.
10. Afterwards, transfer the capillaries to a metal stand and into the preheated furnace for two hrs. This will dry both barrels.
11. After silanization, keep the capillaries dry until use. While the former procedure requires about 3.5 hrs in total, electrodes can now be stored in a desiccator for several weeks.
12. On the day of their experimental use, prepare ion-selective electrodes by filling the tip of the silanized barrel with 1-2 µl of the ion-selective sensor (**Figure 1A**). For potassium-sensitive microelectrodes, use the carrier valinomycin; and for sodium-sensitive microelectrodes, use ETH 157 as carrier.
13. Observe that the ion-selective sensor is quite viscous making it difficult for the tip to fill properly.
14. Fill the reference barrel with HEPES-buffered saline (see below).

NOTE: While other, more simple iso-osmotic saline could be used as well, we prefer to use a saline the composition of which is essentially similar to the perfusion saline (ACSF, see 3.6.), because it may leak out and penetrate into the tissue during experiments. Therefore, it is also essential that this saline does not contain a higher concentration of the ion to be determined than the ACSF used.

15. Backfill the sensor with saline that contains a high concentration of the ion to be detected. Thus, backfill the sensor with 100 mM NaCl saline (for sodium-sensitive microelectrodes) or 100 mM KCl (for potassium-sensitive microelectrodes). Be sure not to insert additional air bubbles during this procedure.
16. If the silanization was successful and the sensor is filled properly, observe the sensor surface form a clearly visible concave surface against the backfill (**Figure 1A**). Otherwise, the sensor may have retracted from the capillary wall and the tip will not be filled. Such electrodes will not be functional.
17. Insert chlorinated silver wires into both barrels (be careful not to touch the sensor) and seal each barrel with dental wax (**Figure 1A**).

2. Preparation of Concentric Ion-selective Microelectrodes

1. For the outer barrel, use thin-walled glass capillaries with filament (outer diameter 2.0 mm) and a length of 7.5 cm. For the inner barrel, take thin-walled capillaries with filament, an outer diameter of 1.2 mm and a length of 10 cm.
2. Clean the capillaries in acetone for 12 hrs. and then rinse several times with abs. ethanol and let them dry. Electrodes can now be stored in a desiccator.
3. Fill approx. 20 ml HMDS into a wide-mouth bottle. CAUTION! HMDS is for use in a fume hood only, vapors are hazardous to health. Close the bottle and put it onto a heating plate, preset to 40 °C. Preheat a furnace, placed under the hood as well, up to 200 °C.
4. Insert the 2.0 mm capillary into a horizontal puller and pull it out to result in capillaries with short tapers and a tip diameter of ~4 µm (**Figure 1B**).
5. Put pulled-out 2.0 mm capillary with its tip up onto a custom-made, special holder (**Figure 2B**, **Figure 2C**) so that its blunt end opens to the cavity of the bottle (**Figure 2C**, right). Afterwards place this holder onto the wide mouth bottle containing the pre-warmed HMDS for 70 min. Make sure that HMDS vapor can flow through all capillaries.
6. Afterwards, transfer the capillaries to a metal stand and into the preheated furnace for two hrs.
7. After silanization, keep the capillaries dry until use. While the former procedure requires about 3.5 hrs in total, now store the electrodes in a desiccator for several weeks.
8. Just before use, fill a small amount of sensor (0.2 µl) into the silanized capillary (**Figure 1B**).
9. To prepare the inner capillary, insert a small diameter capillary into the puller and pull out to result in two capillaries with long tapers and sharp tips (**Figure 1B**). Fill with 100 mM NaCl (sodium-sensitive microelectrodes) or 100 mM KCl (potassium-sensitive microelectrodes) saline.
10. Place the sensor-filled and the saline-filled capillary directly in line with each other onto a custom build stopper made from coverslips. Insert the smaller capillary a short way into the larger capillary.
11. Fix the capillaries onto another coverslip using modeling clay, transfer to the stage of a microscope and visualize using 100x magnification. With help of a glass rod that is mounted on a micromanipulator and by turning the fine drive of the stage of the microscope, slowly advance the outer capillary over the inner capillary until the distance between their tips is roughly 5 µm (**Figure 1B**).
12. Fix the open end of the outer capillary onto the inner capillary using dental wax. Alternatively, apply a small drop of cyanoacrylate (Crazy Glue) instead of wax.
    NOTE: Addition of a small droplet of water will polymerize the glue and fix the electrodes in place. Insert a chlorinated silver wire into the inner barrel and seal it with dental wax (**Figure 1B**).
13. To prepare the reference electrode, take a 7.5 cm long capillary with filament and an outer diameter of 1.5 mm and pull out with a vertical puller. Ensure that the tips are relatively long but not too sharp (tip diameter ~1 µm).
14. Discard the upper pipette, open the lower chuck and lift the lower pipette by about 5 mm. Close the chuck again and lift it until the tip of the lower electrode is positioned about 5 mm above the heating coil. Heat the coil and use forceps to bend the tip by about 45° to the side. Lower pipette about 1-2 mm. Bend again by about -45° to direct the tip back in parallel to the main shaft (**Figure 1B**). This procedure is necessary to enable the close positioning of the tip of the reference electrode to the concentric electrode.
15. Fill the reference barrel with HEPES-buffered saline (see below), insert a chlorinated silver wire and seal the barrel with dental wax (**Figure 1B**).

3. Salines

1. Prepare saline for backfill of potassium-sensitive electrodes (see 1.15.) composed of 100 mM KCl. Saline for backfill of sodium- sensitive electrodes is composed of 100 mM NaCl.
2. Prepare saline for backfill of reference barrels (HEPES-buffered saline, see 1.16.) is composed of (in mM): 125 NaCl, 2.5 KCl, 2 $CaCl_2$, 2 $MgSO_4$, 1.25 NaH_2PO_4, and 25 HEPES , titrated with NaOH to result in a pH of 7.4.
3. Prepare saline for calibration of potassium-sensitive electrodes are composed of 25 mM HEPES and a total of 150 mM NaCl and KCl, pH adjusted to 7.4 with NMDG-OH (N-methyl-D-glucamine). Here, calibration was performed with salines containing 1, 2, 4 or 10 mM KCl; ACSF contained 2.5 mM KCl (**Figure 5**).
4. Prepare saline for calibration of sodium-sensitive electrodes as follows; (in mM) 25 HEPES, 3 KCl, a total of 160 NaCl and NMDG-Cl, pH adjusted to 7.4 with NMDG-OH. Perform calibration with saline containing (in mM) 70, 100, 130 or 160 NaCl; ACSF contained 152 NaCl (**Figure 6**).
5. For determination of cross-reaction of the sensor with other ions, *e.g.*, pH, prepare additional calibration salines with fixed ion concentrations, but varying pH.
    NOTE: While this procedure is not demonstrated in the present study, please should refer to earlier work addressing this issue (*e.g.* [11,12]).
6. Prepare acute brain tissue slices in saline composed of (in mM): 125 NaCl, 2.5 KCl, 0.5 $CaCl_2$, 6 $MgCl_2$, 1.25 NaH_2PO_4, 26 $NaHCO_3$, and 20 glucose, bubbled with 95% O_2 and 5% CO_2, resulting in a pH of 7.4.
7. Perform experiments in brain slices in artificial cerebrospinal fluid (ACSF) composed of (in mM): 125 NaCl, 2.5 KCl, 2 $CaCl_2$, 1 $MgCl_2$, 1.25 NaH_2PO_4, 26 $NaHCO_3$, and 20 glucose, bubbled with 95% O_2 and 5% CO2, resulting in a pH of 7.4.

8. For stimulation of neurons and glial cells, prepare solutions containing 0.2, 0.3, 0.4 or 0.5 mM glutamate or 10 mM L-aspartate dissolved in ACSF. For pressure application, dissolve 10 mM glutamate in HEPES-buffered saline.
9. Prepare application pipette for pressure application. Insert thin-walled glass capillaries with filament (outer diameter 2.0 mm) and a length of 7.5 cm into horizontal puller and pull out to result in a tip diameter of ~ 1 µM.
10. For induction of epileptiform activity, prepare magnesium-free ACSF containing 10 µM bicuculline methiodide.
11. To inhibit the generation of action potentials, prepare a 10 mM stock solution of tetrodotoxin (TTX) in distilled water. During experiments, TTX is directly added to the ACSF to result in a final concentration of 0.5 µM.
12. To prevent activation of AMPA-receptors, prepare a 50 mM stock solution of cyano-nitroquinoxaline-dione (CNQX) in dimethyl sulfoxide (DMSO). During experiments, this is directly added to the ACSF to result in a final concentration of 100 µM.
13. To block activation of NMDA-receptors, prepare a 50 mM stock solution of amino-phosphonopentanoate (APV) in 70 mM $NaHCO_3$. During experiments, this is directly added to the ACSF to result in a final concentration of 100 µM.

4. Calibration of Ion-selective Microelectrodes

1. Calibrate ion-selective microelectrode directly before and after each experiment.
2. Attach electrodes to micromanipulators and insert them into an ACSF-perfused experimental chamber, placed under a stereo microscope (**Figure 3**, **4**). Place the reference electrode into the pre-chamber (**Figure 4A**, **B**). Switch on bath perfusion, ensure that the flow is about 2 ml/min.

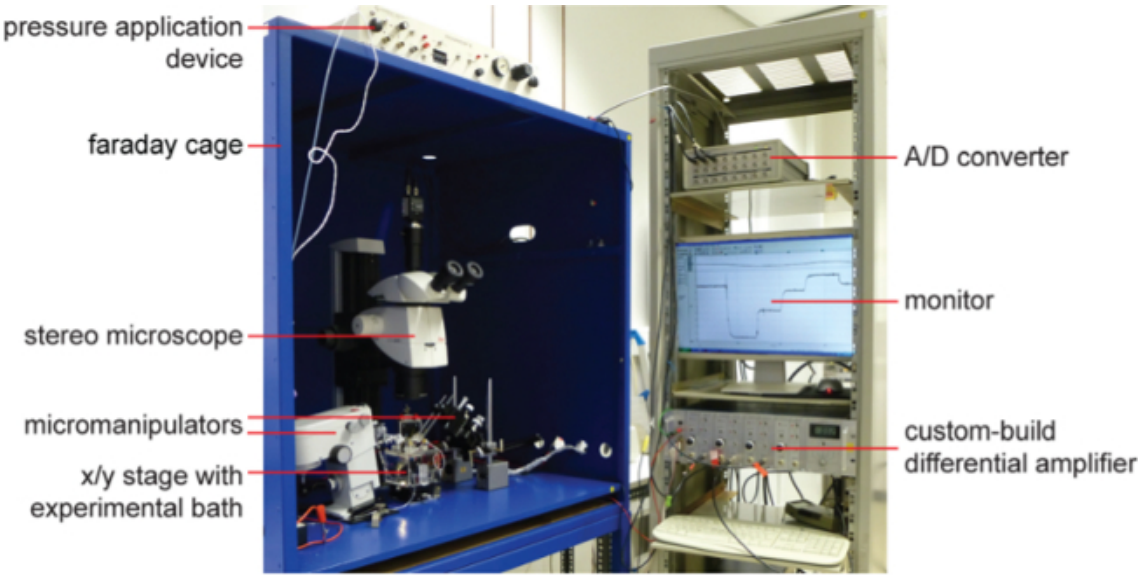

Figure 3. The experimental work space. The recording rig consists of a vibration-damped table carrying the x/y-translational stage with the experimental bath, the micromanipulators, and a stereomicroscope with high quality optics. The stereo microscope is also equipped with a CCD camera for documentation purposes. In addition, a pressure application device for focal drug application is used. The recording electrodes are coupled via the head stage to a differential amplifier. The digitized data (A/D converter) is recorded with a computer. The bath perfusion is realized by a peristaltic micro pump (not shown). Please click here to view a larger version of this figure.

3. Switch on the A/D converter, the differential amplifier, and the computer, and start the recording software (**Figure 3**, **4**). Because resistance of the ion-sensitive barrels is very high (10-20 GΩ; see below), use a special electrometer amplifier with high input impedance (R_{in}= 10 TΩ) and a small bias current (I_{bias}= 50 fA - 1 pA).

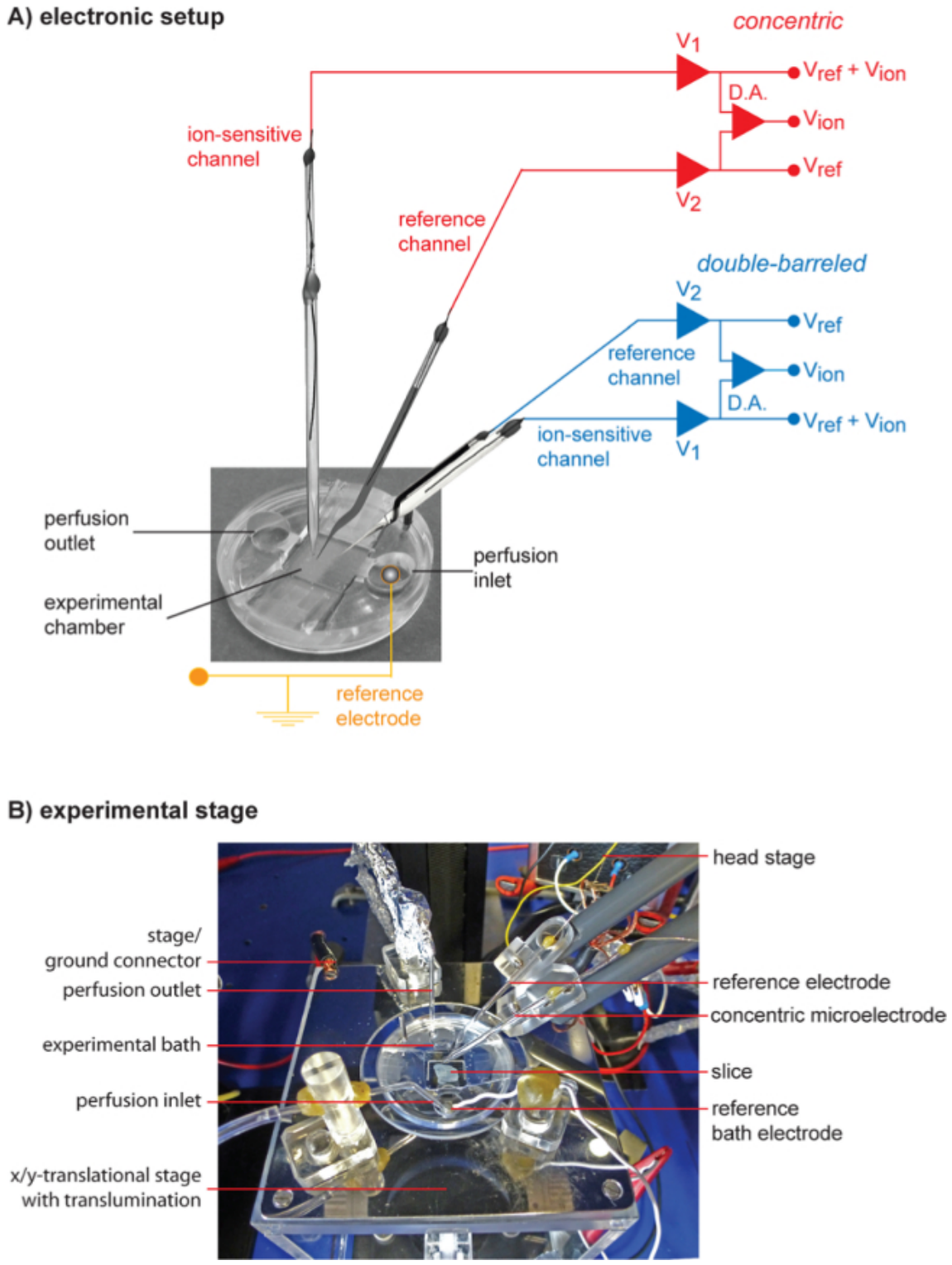

Figure 4. Electronic and spatial design of the experimental setup. (**A**) Schematic view of the recording arrangement. The tips of a double-barreled microelectrode (blue) and a concentric microelectrode (red) are arranged in an experimental bath filled with saline. The bath reference electrode is indicated schematically. The potential detected by the ion-selective barrels (V_1) is composed of the electrical field potential (V_{ref}) and the ion potential (V_{ion}), whereas the reference barrels (V_2) only detect V_{ref}. To isolate V_{ion}, V_{ref} is subtracted from V_1 by means of a differential amplifier (D.A.). (**B**) Topography of the experimental stage with a concentric microelectrode in place. The center of the experimental stage consists of the experimental bath containing the slice preparation. To ground the bath, the reference bath electrode is submerged in the pre-chamber which also hosts the perfusion inlet. The stage itself is grounded by a separate ground connector. The concentric microelectrode and its reference electrode are carried by separate pipette holders driven by micromanipulators. Microelectrode and reference electrode are electronically coupled to the head stage of the amplifier. Please click here to view a larger version of this figure.

4. Connect chlorinated silver wires to the respective inputs of the head stage of the differential amplifier (**Figure 4**). Determine electrode resistances. Ensure that the resistance of the reference barrel is between 30-100 MΩ and the resistance of the ion-sensitive barrel is between 10-20 GΩ.
5. Adjust voltage signals to zero and start recording.
6. Note that the potential detected by the ion-selective barrels (V_1) is composed of the electrical field potential (V_{ref}) and the ion potential (V_{ion}), whereas the reference barrels (V_2) only detect V_{ref}. To isolate V_{ion}, V_{ref} is subtracted from V_1 by means of a differential amplifier (D.A.) (**Figure 4A**).
7. After obtaining a stable baseline, switch to calibration salines containing defined concentrations of the ion to be measured.
   NOTE: **Figure 5A** shows the calibration of a double-barreled potassium-sensitive microelectrode. In **Figure 6A**, the calibration of both a double-barreled as well as a concentric Na^+-sensitive microelectrode is shown. While we do not describe the procedure here, note that possible interferences with other ions must be tested before using a specific ionophore (see also 3.4.).

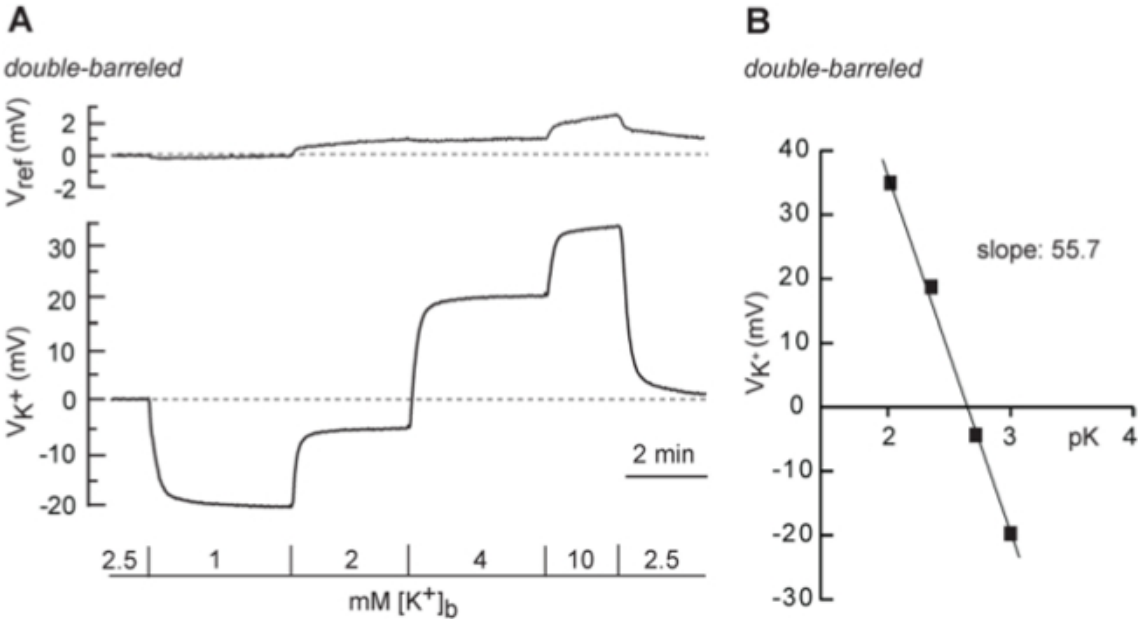

Figure 5. Calibration of double-barreled potassium-selective microelectrodes. (**A**) Change in the voltage of the reference barrel (V_{ref}) and of the K^+-potential (V_{K+}) in response to changes in the bath K^+ concentration ($[K^+]_b$) as indicated. (**B**) Half-logarithmic plot of $[K^+]_b$ versus V_{K+}. A linear plot of the data reveals a slope of about 56 mV. For illustration purposes, traces were smoothed with a Sawitzky-Golay filter (width 20). Please click here to view a larger version of this figure.

8. Determine the voltage response of the ion-selective barrel in response to a known change in ion concentration. Plot data in a single logarithmic plot (**Figure 5B**, **6B**) and determine the slope. An ideal sensor follows a relationship described by the Nernst equation (see e. g. [13]):

$$V = V_0 + \frac{R \times T}{z \times F} \times \ln \frac{c'}{c''}$$

Equation 1

V: measured electrode potential;
V_0: standard electrode potential, e. g. for a AgCl-wire at a temperature of 298.15 K and a partial pressure of 101.325 kPa (absolute)
R: gas constant (8.314 joules/degree Kelvin/mole)
T: absolute temperature (in Kelvin)
z: charge on the ion (+ 1 for potassium and sodium)
F: Faraday constant (96.500 coulombs)
c': extracellular ion concentration
c'': intracellular ion concentration

For practical purposes, and the natural logarithm are converted to the Nernst slope *s* which is then valid for a given ion and temperature:

$$V = V_0 + s \times \log \frac{c'}{c''}$$

Equation 2

NOTE: For potassium and sodium electrodes, an ideal voltage response of the sensor thus exhibits a linear slope of about -58 mV at RT. Some deviation of this can be accepted (**Figure 5B**, **6B**). It is essential, however, that response characteristics of a given electrode do not change significantly (by more than 10%, see below) before and after an experiment.

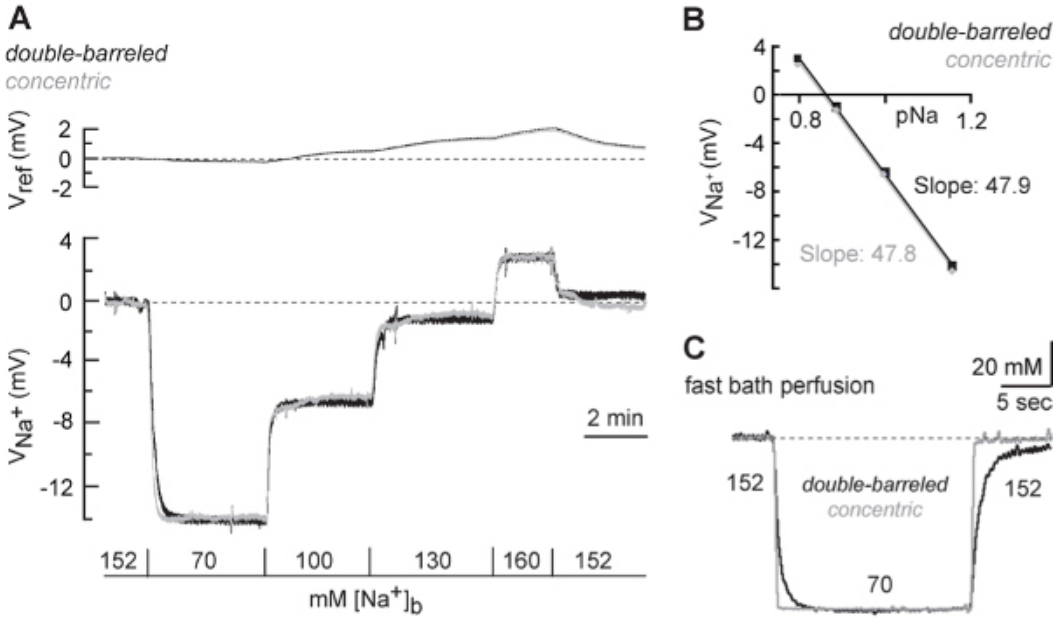

Figure 6. Calibration of sodium-selective microelectrodes and comparison of double-barreled with concentric electrodes. (**A**) Top traces: Change in the voltage of the reference barrels (V_{ref}) of a double-barreled electrode (black dotted trace) and a concentric electrode (gray trace) in response to changes in the bath Na^+ concentration ($[Na^+]_b$) as indicated. Note that the voltage responses of both electrodes are virtually identical. Bottom traces: Changes in the voltage of the Na^+-potential (V_{Na+}) of a double-barreled electrode (black trace) and a concentric electrode (grey trace) in response to changes in $[Na^+]_b$. (**B**) Half-logarithmic plots of the $[Na^+]_b$ versus the V_{Na+} of both electrodes. Linear plots of the data reveal a slope of about 48 mV for both electrodes. (**C**) Response of the V_{Na+} of a double-barreled (black trace) and a concentric electrode (gray trace) to a fast change in the $[Na^+]_b$ from 152 mM to 70 mM. Note that the response time of the concentric electrode is significantly faster. For illustration purposes, traces were smoothed with a Sawitzky-Golay filter (width 20). Please click here to view a larger version of this figure.

9. Determine the response time of the electrodes, which depends on the tip diameter, the form of the tip as well as on the thickness of the sensor phase in the electrode tip.
   NOTE: In this experimental set up and employing a rapid change between different perfusion salines (exchange completed at the electrode's tip within 500 msec), double-barreled sodium-sensitive microelectrodes reached a stable potential within 9.7 ± 4.5 sec when switching from 152 mM to 70 mM $[Na^+]$ (n=6). Within the same setting, concentric sodium-sensitive microelectrodes reached a stable potential within only 0.8 ± 0.3 sec (n=6) (**Figure 6C**). This emphasizes the superior time resolution of concentric as compared to double-barreled microelectrodes.

5. Dissection of Tissue

1. For generation of acute slices, anaesthetize mice of postnatal days 16-20 with CO_2 and quickly decapitated (following the recommendation of the European Commission published in: Euthanasia of experimental animals, Luxembourg: Office for Official Publications of the European Communities, 1997; ISBN 92–827-9694-9).
2. Prepare hippocampal tissue slices (thickness 250 µm), following a standard procedure (see e. g. [14]).

6. Experimental Procedures

1. Transfer a slice into the experimental chamber and fix it with a grid.
2. Lower the calibrated ion-selective microelectrode onto the slice surface and impale the *stratum radiatum* of the CA1 region to a depth of about 50 µm with the electrode.
   NOTE: Touching the slice surface with the microelectrode leads to characteristic fluctuations in the ion-sensitive barrel. Furthermore, damage to cells during impalement of the tissue causes fluctuations as well. Wait until baseline has stabilized.
3. For pressure application of transmitter agonists, fill an application pipette with compound (e. g. 0.5 mM glutamate). Attach the pipette to a micromanipulator and couple it to a pressure application device.
4. Lower application pipette into the tissue and carefully place it in the proximity of the tip of the ion-selective microelectrode (~20-40 µm). Start pressure application (e. g. 10 sec, 40 mbar) and record voltage changes as monitored by the ion-selective microelectrode.

5. For bath application of drugs, switch between different perfusion salines for a defined duration.
6. To terminate the experiment, carefully withdraw the ion-selective microelectrode from the tissue and record any drift in potentials from the original zero value that might have occurred during prolonged recording periods.
7. Remove slice preparation from the bath and perform a second calibration of the ion-selective microelectrode.
   NOTE: This is necessary because the electrode tip can get clogged during its movement through the tissue. Thus, it is essential to ensure that the electrode still responds properly to changes in ion concentrations. Experiments should be rejected if the electrode's response to a ten-fold change in ion concentration has dropped by more than 10%. Well-working electrodes can in principle be re-used in several experiments. This is especially true for concentric electrodes, which can even last for several days. It is essential, however, that calibration procedures are repeated before and after each single experiment to ensure the proper functioning of the electrodes.

7. Data Analysis

1. To convert the voltage response of the ion-selective electrode to changes in extracellular ion concentration, first convert equation 2 to determine the change in the potential ΔV_{ion} (mV) as follows (demonstrated here for K^+-sensitive electrodes, analog procedure applies for Na^+-sensitive electrodes):

$$\Delta V_{K^+} = s \times log \frac{[K^+]_B + \Delta[K^+]_o}{[K^+]_B}$$

Equation 3

V_{K+}: changes in the potential of the valinomycin barrel (mV)

s: Nernst slope

$K^+]_B$: baseline concentration of potassium (in our case 2.5 mM K^+)

$K^+]_o$: changes in $[K^+]_o$ during experiment

2. Calculate the arithmetic average of the slopes derived from the single logarithmic plots of the calibration before and after the experiment (cf. **Figure 5B, 6B**; see point 4.8) to retrieve "s".
3. To calculate changes the $[K^+]_o$ ($\Delta[K^+]_o$, in mM), rearrange equation 3 to:

$$\Delta[K^+]_o = [K^+]_B \times \left(10^{\frac{\Delta V_{K^+}}{s}} - 1\right)$$

Equation 4

Representative Results

To monitor $[K^+]_o$ and changes therein in response to excitatory activity, a double-barreled potassium-selective microelectrode was inserted into the *stratum radiatum* of the CA1 area. A few minutes after impalement, the ion-selective barrel of the electrode reached a stable baseline (**Figure 7A**), corresponding to a $[K^+]_o$ of about 2.8 mM, a value close to the $[K^+]$ of the ACSF used (2.5 mM). Bath application of 0.5 mM glutamate for 10 sec induced a reversible increase in $[K^+]_o$ by about 4 mM, followed by an undershoot below baseline amounting to ~0.7 mM (**Figure 7A**). Lowering the glutamate concentration to 0.4, 0.3, and 0.2 mM caused a corresponding reduction in the amplitude of both the transient increase and the undershoot in $[K^+]_o$ (**Figure 7A**).

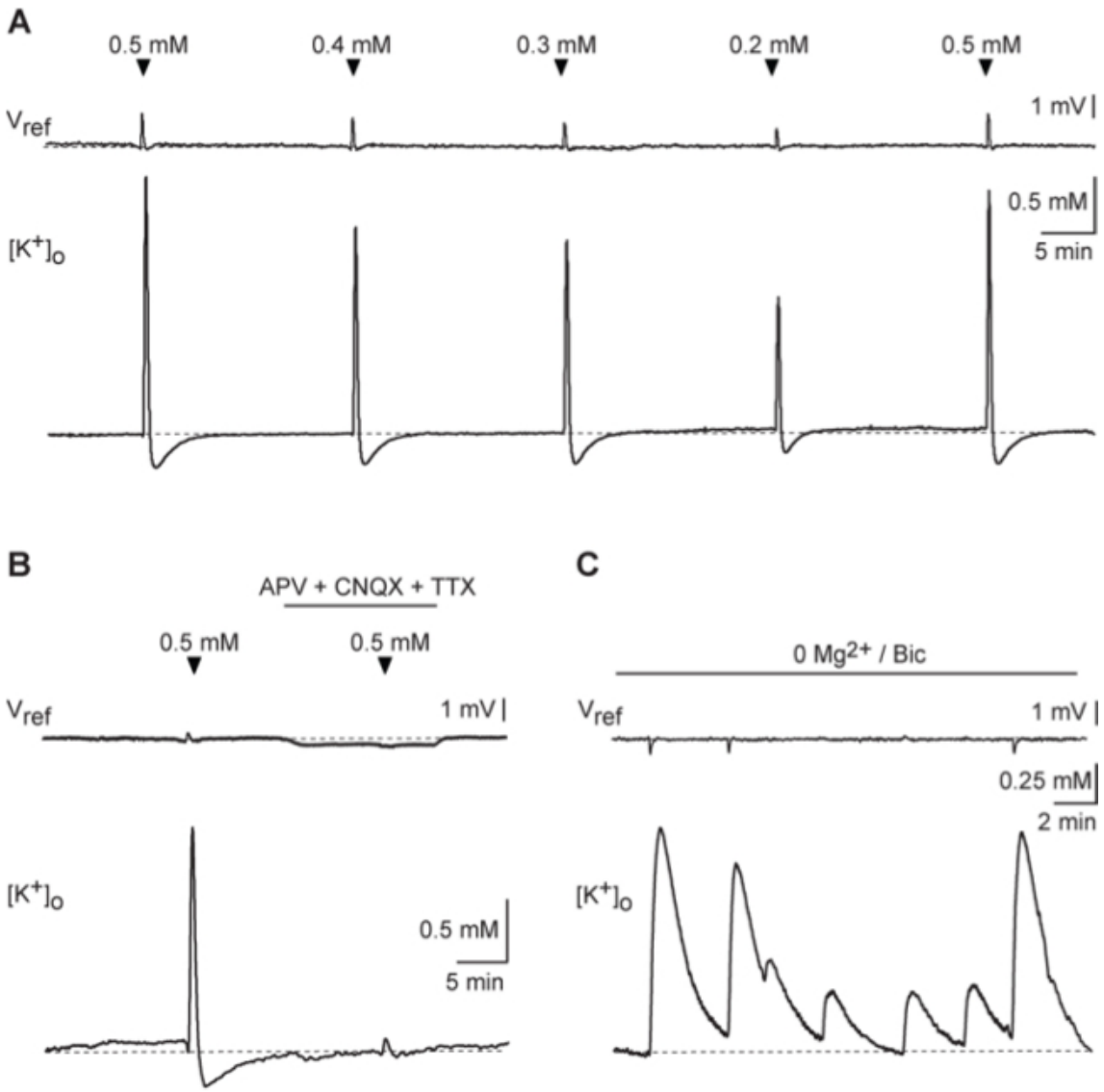

Figure 7. Extracellular potassium transients inresponse to excitatory activity. (**A**) $[K^+]_o$ transients, consisting of an increase followed by an undershoot below baseline, induced by bath application of different concentrations of glutamate for 10 sec as indicated. (**B**) Influence of a perfusion with glutamate receptor blockers (CNQX, 100 µM; APV, 100 µM) and tetrodotoxin (TTX; 0.5 µM) on $[K^+]_o$ transients induced by bath application of 0.5 mM glutamate for 10 sec. (**C**) Spontaneous $[K^+]_o$ transients in the presence of $0Mg^{2+}$/BIC. Experiments shown in A-C were performed using double-barreled electrodes. For illustration purposes, traces were smoothed with a Sawitzky-Golay filter (width 20). Please click here to view a larger version of this figure.

Earlier experiments have shown that such glutamate-induced $[K^+]_o$ signals are not significantly altered during application of TTX, and are thus largely independent on the opening of voltage-gated sodium channels and neuronal action potential generation [15,16]. To study the mechanisms underlying the observed $[K^+]_o$ changes in response to glutamate, we applied glutamate receptor blockers, namely CNQX (100 µM; blocker of AMPA receptors) and APV (100 µM; blocker of NMDA receptors) in the presence of TTX (0.5 µM). Upon bath perfusion with these blockers, glutamate-induced $[K^+]_o$ changes were virtually abolished, confirming their dependence on the opening of ionotropic glutamate receptor channels as reported before (*e.g.* [17]; **Figure 7B**).

To further demonstrate the relevance of glutamatergic excitation for the generation of extracellular $[K^+]$ signals, slices were perfused with nominally Mg^{2+}-free saline containing 10 µM bicuculline methiodide ($0Mg^{2+}$/BIC). This relieves voltage-dependent Mg^{2+}-block of NMDA receptors and dampens inhibition by blocking $GABA_A$ receptors, causing spontaneous recurrent epileptiform activity in the network (*e.g.* [18,19]). As expected [20], spontaneous, recurrent $[K^+]_o$ transients, amounting to about 1.5 mM were detected in $0Mg^{2+}$/BIC saline (**Figure 7C**). In between these responses, smaller $[K^+]_o$ transients with a mean amplitude of about 0.2 mM occurred (**Figure 7C**).

In a second set of experiments, we used $[Na^+]$-sensitive microelectrodes to determine $[Na^+]_o$ changes evoked by application of glutamate agonists. Here, we also compared the response characteristics of double-barreled and concentric microelectrodes employing two different application paradigms. $[Na^+]$-sensitive microelectrodes were positioned into the *stratum radiatum* at a depth of about 50 µM. After a stable baseline was attained, the glutamate agonist L-aspartate was applied per bath perfusion (10 mM, 120 sec, bath perfusion at 2.5 ml/min). As observed earlier [21], application of aspartate caused a slow decrease in $[Na^+]_o$ by roughly 15 mM, which lasted about 5 min and then started to

recover back to baseline (**Figure 8A**). Notably, while the peak amplitudes and kinetics of the $[Na^+]_o$ signals determined by both electrodes were virtually identical under these conditions, concentric electrodes exhibited a more stable baseline and a lower noise level (**Figure 8A**).

To test the response characteristics of the different electrodes under a more rapid application paradigm, we pressure-applied glutamate through a fine glass pipette positioned in the *stratum radiatum* at a distance of 20-40 µm from the tip of the ion-selective microelectrode. As expected [21], application of glutamate (10 mM) for 200 ms caused a drop in the $[Na^+]_o$ (**Figure 8B**). The peak amplitudes of the $[Na^+]_o$ decrease were in the same range for both types of electrodes (double barreled: 4.5 - 13.5 mM, n=14; concentric: 2.0 - 19.1 mM, n=15). However, in contrast to the results obtained with slow bath perfusion (see above), not only the signal-to-noise ratio, but also the time course of the $[Na^+]_o$ signals detected by the two types of electrodes differed significantly. The average time to peak was 3.5 sec for the double-barreled and only 1.3 sec for the concentric microelectrodes.

Thus, these results demonstrate and confirm the faster response kinetics of concentric vs. double-barreled Na^+-selective microelectrodes, (cf. **Figure 6C and 8B**), as was also noted for Ca^{2+} and pH-selective counterparts [10]. In contrast to the former study, in which short-burst synaptic stimulation was performed to evoke fast synaptically-induced ion transients, there was only a tendency, but no significant difference in mean peak amplitudes between concentric and double-barreled electrodes with our application paradigm. This was probably due to the fact that the distance of the application pipette from the tip of the ion-selective microelectrode varied by a factor of two (20-40 µm), and consequently, that the maximal glutamate concentration at the target region was not the same in different experiments, obstructing any existing difference in peak amplitudes.

(A) Top traces: Change in the voltage of the reference barrels (V_{ref}) of a double-barreled electrode (black dotted trace) and a concentric electrode (gray trace) in response to changes in the bath Na^+ concentration ($[Na^+]_b$) as indicated. Note that the voltage responses of both electrodes are virtually identical. Bottom traces: Changes in the voltage of the Na^+-potential (V_{Na+}) of a double-barreled electrode (black trace) and a concentric electrode (grey trace) in response to changes in $[Na^+]_b$. (B) Half-logarithmic plots of the $[Na^+]_b$ versus the V_{Na+} of both electrodes. Linear plots of the data reveal a slope of about 48 mV for both electrodes. (C) Response of the V_{Na+} of a double-barreled (black trace) and a concentric electrode (gray trace) to a fast change in the $[Na^+]_b$ from 152 mM to 70 mM. Note that the response time of the concentric electrode is significantly faster. For illustration purposes, traces were smoothed with a Sawitzky-Golay filter (width 20).

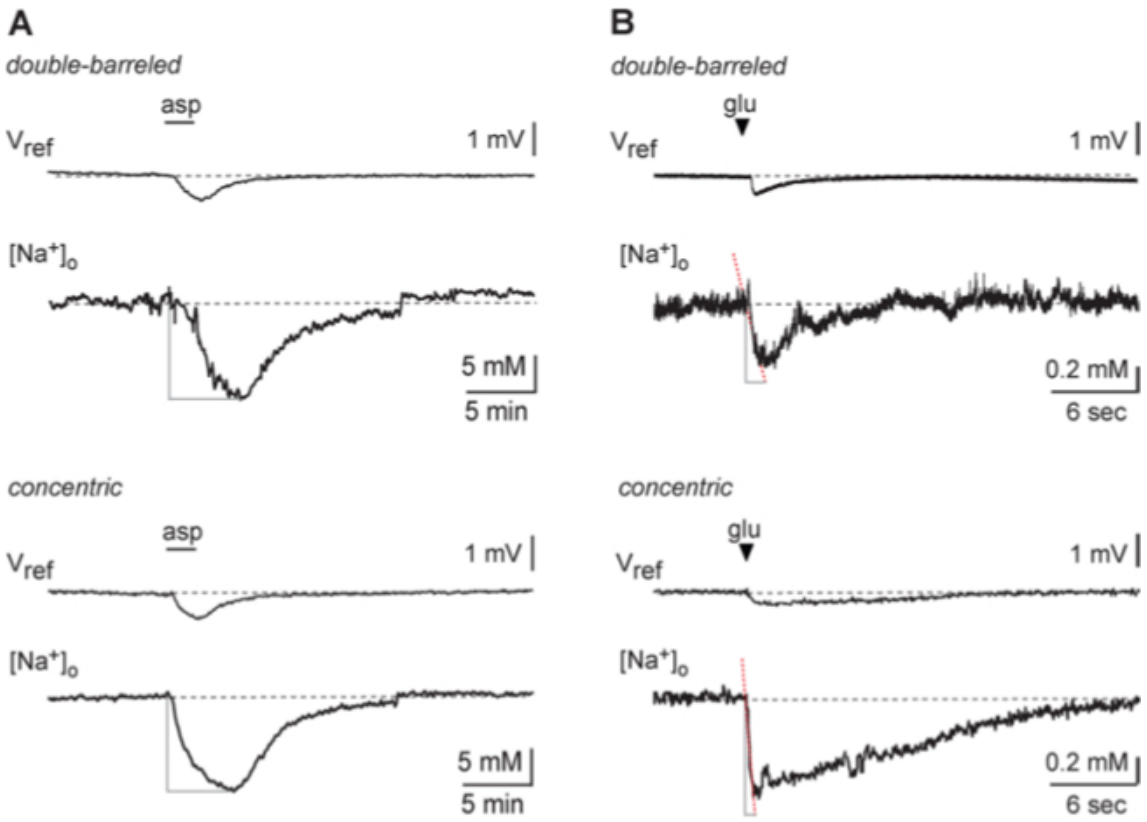

Figure 8: Extracellular sodium transients as detected by double-barreled and concentric electrodes.
(**A**) Transient changes in V_{ref} and $[Na^+]_o$ induced by bath perfusion with 10 mM aspartate for 120 sec as indicated by the bar. The upper traces show a recording performed with a double-barreled electrode, the lower traces were recorded using a concentric electrode. (**B**) Transient changes in V_{ref} and $[Na^+]_o$ induced by local pressure application with 10 mM glutamate for 0.2 sec as indicated by the arrowhead. The upper traces show a recording performed with a double-barreled electrode, the lower traces were recorded using a concentric electrode. Dotted red lines represent linear fits of the period between the start of the signal to its maximum. Note that the response time of the concentric electrode is significantly faster under this condition. For illustration purposes, traces were smoothed with a Sawitzky-Golay filter (width 20). Please click here to view a larger version of this figure.

Discussion

Liquid-carrier-based, ion-selective electrodes have been successfully employed for decades and for many ions, highly specific sensors are available [22-26]. When used in the extracellular space (ECS) of vertebrate brain preparations, one must keep in mind, however, that this is a quite invasive technique: while the width of the ECS is only around 20-50 nm, the diameter of ion-selective microelectrodes is about 1 µm (double-barreled electrodes) or larger (concentric electrodes). The tips of ion-selective microelectrodes will thus not only damage tissue during their impalement of the tissue, but also enlarge the ECS, favouring an underestimation of ion transients. Despite these pitfalls, extracellular ion transients in response to neuronal activity are remarkably consistent between different laboratories [7,8], attesting to the reliability of this method.

The performance and suitability of ion-selective electrodes is dependent on their sensitivity and selectivity, which is defined by the sensor cocktail ('liquid membrane ionophore') used. Sensor cocktails contain a special carrier molecule, *e.g.* valinomycin for K^+-selective microelectrodes which exhibits a high selectivity for potassium [27]. Notwithstanding, cross-reactivity with other ions can occur and must be tested. Valinomycin exhibits a significant cross-reactivity for ammonium, which has to be considered when interpreting results (*e.g.* [11,12]). Furthermore, because the voltage-response of the ionophores follows a Nernstian behavior (cf. equation 1), the signal-to-noise ratio and detection threshold depend on the concentration of the ion to be measured. Thus, while small $[K^+]_o$ transients evoke large voltage changes against the low baseline $[K^+]_o$, small $[Na^+]_o$ transients are much more difficult to detect against the high baseline $[Na^+]_o$ (cf. **Figure 5 and 6**).

The performance of ion-selective electrodes is also determined by the temporal resolution, which is largely governed by its electrical time constant. The latter is mainly determined by the axial resistance of the sensor, and by the distributed capacitance along the length of the pipette, between its internal solutions and the external fluid. In the double-barreled configuration, the resistance is high, owing to the long column of backfilled ion sensor. For a given insulating dielectric (in this case borosilicate glass), the capacitance is governed by the dielectric thickness. In double-barreled electrodes, the dielectric width amounts to the glass wall of the pipette. As the glass thins close to the tip, the dielectric width falls, and the capacitance increases. These factors combine to produce electrodes with response times that range from several hundred milliseconds to several seconds, as these factors are varied.

A major advantage of the concentric design is that both the axial resistance and the capacitance to the bath are greatly diminished. The concentric pipette shunts most of the resistance of the backfilled ion exchanger, leaving only a remnant in the last few micrometers before the tip. In addition, the filling solution within the concentric pipette is physically distanced from the bath, separated by the thickness of two glass walls, greatly reducing the capacitance. As shown earlier [10], the combined effect of reduced resistance and capacitance is an improvement in temporal resolution of two orders of magnitude. In the case of concentric Ca^{2+} and pH microelectrodes, 90% response times were as low as 10-20 msec [10]. A related advantage of the concentric design is the lower noise level (cf. **Figure 8**). Owing to the greatly reduced resistance, voltage transients from any ambient noise are minimized. Moreover, recovery from such transients is rapid, because of the fast time constant. Such artifacts are therefore small and fast, and have a less disruptive effect on physiological recordings (cf. **Figure 8**).

There are also disadvantages of the concentric technique. First, their assembly is more complex, and time-consuming. A second disadvantage is the need to place a separate reference microelectrode with its tip, entailing use of either a separate micromanipulator or a specialized dual manipulator. Finally, double-barreled microelectrodes can be extended to a triple-barreled design, allowing detection of two different ion species at the same time [28], which is not possible for concentric electrodes.

Most common pitfalls

Inefficient silanization.

The most important step, and principal obstacle in fabrication of any liquid-sensor based ion-selective microelectrode is the silanization procedure. When electrodes fail to respond to changes in specific ion concentration, or respond with a sub-Nernstian response (*i.e.*, well less than 58 mV per ten-fold concentration difference), poor efficacy of silanization is typically the cause. In our experience, this can occur if atmospheric humidity is too high, or too low, typical of conditions at the height of summer, or winter, respectively. If it is feasible to exert some control over room humidity, these problems may be overcome.

Electrode resistance is too high.

If needed, the resistance of the ion-sensitive barrel can be reduced by bevelling. To this end, expose its tip to a strong jet of an abrasive suspended in water for a couple of seconds. This will cause its upmost tip to break and lower the resistance to the desired value.

Salt bridges.

Salt bridges between the ion and reference barrels result in poorly or none-responding electrodes and can thus also greatly confound their performance in the calibration. As mentioned above (see point 1.6.), this is mainly an issue when double-barreled theta glass is chosen, but is a rare occurrence when using the offset, twisted barrel technique described here.

With ease of fabrication in mind, the original double-barreled design of Lux [29] can often be used profitably. This method utilizes pre-filling of the ion and reference barrels with salt solutions, a fast exposure to a silane solution by its suction and expulsion from the tip, following by incorporation of ion-exchanger, also via the tip (see [30,31]). These electrodes can be fabricated in roughly 10 min, but their tip size is typically 4 µm or more and they are more prone to fail during an experiment. In contrast, silanization methods that involve exposure to silane vapor and heating can produce electrodes with smaller tips that last days, and sometimes weeks.

Taken together, there are several protocols and approaches on how to prepare ion-selective microelectrodes. Here, we have described two main procedures for fabrication of twisted double-barreled as well as concentric microelectrodes which work well and reliably in our laboratories, with an overall success rate of close to 100%. Importantly, these techniques will be transferable to measurement of other ions species, including pH or calcium, and will also be applicable to other preparations than the brain, including fluid-filled cavities or fluids in general. Last, but not least,

ion-selective microelectrodes allow determination of ion concentrations inside cells. Because of their relatively large tip size (~ 1 µm), this will, however, be possible only in cells with a large cell body, *e.g.* such as found in invertebrate preparations [28,32].

Disclosures

The authors declare no competing interests.

Acknowledgements

The authors wish to thank C. Roderigo for expert technical assistance. We thank S. Köhler (Center of Advanced Imaging, Heinrich Heine University Duesseldorf) for help in video production. Research in the author's laboratory has been funded by the German Research Association (DFG: Ro 2327/8-1 to CRR), the Heinrich Heine University Duesseldorf (to NH) and by National Institutes of Health grant R01NS032123 (to MC).

References

1. Somjen, G. G. Ion regulation in the brain: implications for pathophysiology. *Neuroscientist.* **8**, 254-267 (2002).
2. Dietzel, I., Heinemann, U., Hofmeier, G., Lux, H. D. Stimulus-induced changes in extracellular Na+ and Cl- concentration in relation to changes in the size of the extracellular space. *Exp Brain Res.* **46**, 73-84 (1982).
3. Nicholson, C., ten Bruggencate, G., Stockle, H., Steinberg, R. Calcium and potassium changes in extracellular microenvironment of cat cerebellar cortex. *J Neurophysiol.* **41**, 1026-1039 (1978).
4. Rice, M. E., Nicholson, C. Glutamate- and aspartate-induced extracellular potassium and calcium shifts and their relation to those of kainate, quisqualate and N-methyl-D-aspartate in the isolated turtle cerebellum. *Neuroscience.* **38**, 295-310 (1990).
5. Prince, D. A., Lux, H. D., Neher, E. Measurement of extracellular potassium activity in cat cortex. *Brain Res.* **50**, 489-495 (1973).
6. Deitmer, J. W., Rose, C. R. pH regulation and proton signalling by glial cells. *Prog Neurobiol.* **48**, 73-103 (1996).
7. Chesler, M. Regulation and modulation of pH in the brain. *Physiol Rev.* **83**, 1183-1221 (2003).
8. Kofuji, P., Newman, E. *Regulation of potassium by glial cells in the central nervous system.* Springer (2009).
9. Nicholson, C. Ion-selective microelectrodes and diffusion measurements as tools to explore the brain cell microenvironment. *J Neurosci Methods.* **48**, 199-213 (1993).
10. Fedirko, N., Svichar, N., Chesler, M. Fabrication and use of high-speed, concentric h+- and Ca2+-selective microelectrodes suitable for in vitro extracellular recording. *J Neurophysiol.* **96**, 919-924 (2006).
11. Stephan, J., *et al.* Kir4.1 channels mediate a depolarization of hippocampal astrocytes under hyperammonemic conditions in situ. *Glia.* **60**, 965-978 (2012).
12. Haack, N., Rose, C. R. Preparation, Calibration and Application of Potassium-Selective Microelectrodes. *Microelectrodes.* Lei, K. F. 87-105 Nova Science Publishers (2014).
13. Roos, A., Boron, W. F. Intracellular pH. *Physiol Rev.* **61**, 296-434 (1981).
14. Kleinhans, C., Kafitz, K. W., Rose, C. R. Multi-photon Intracellular Sodium Imaging Combined with UV-mediated Focal Uncaging of Glutamate in CA1 Pyramidal Neurons. *Journal of visualized experiments : JoVE.* (2014).
15. Hertz, L., *et al.* Roles of astrocytic Na ,K -ATPase and glycogenolysis for K homeostasis in mammalian brain. *J Neurosci Res.* (2014).
16. Pumain, R., Heinemann, U. Stimulus- and amino acid-induced calcium and potassium changes in rat neocortex. *J Neurophysiol.* **53**, 1-16 (1985).
17. Vargova, L., Jendelova, P., Chvatal, A., Sykova, E. Glutamate, AMPA, NMDA Induced Changes in Extracellular Space Volume and Tortuosity in the Rat Spinal Cord. *J Cereb Blood Flow Metab.* **21**, 1077-1089 (2001).
18. Fellin, T., Gomez-Gonzalo, M., Gobbo, S., Carmignoto, G., Haydon, P. G. Astrocytic glutamate is not necessary for the generation of epileptiform neuronal activity in hippocampal slices. *J Neurosci.* **26**, 9312-9322 (2006).
19. Rouach, N., Koulakoff, A., Abudara, V., Willecke, K., Giaume, C. Astroglial metabolic networks sustain hippocampal synaptic transmission. *Science.* **322**, 1551-1555 (2008).
20. Lux, H. D., Heinemann, U., Dietzel, I. Ionic changes and alterations in the size of the extracellular space during epileptic activity. *Adv Neurol.* **44**, 619-639 (1986).
21. Zanotto, L., Heinemann, U. Aspartate and glutamate induced reductions in extracellular free calcium and sodium concentration in area CA1 of 'in vitro' hippocampal slices of rats. *Neurosci Lett.* **35**, 79-84 (1983).
22. Borrelli, M. J., Carlini, W. G., Dewey, W. C., Ransom, B. R. A simple method for making ion-selective microelectrodes suitable for intracellular recording in vertebrate cells. *J Neurosci Methods.* **15**, 141-154 (1985).
23. Ammann, D., Anker, P. Neutral carrier sodium ion-selective microelectrode for extracellular studies. *Neurosci Lett.* **57**, 267-271 (1985).
24. Deitmer, J. W., Schlue, W. R. Intracellular Na+ and Ca2+ in leech Retzius neurones during inhibition of the Na+-K+ pump. *Pflugers Arch.* **397**, 195-201 (1983).
25. Schwiening, C. J., Thomas, R. C. Relationship between intracellular calcium and its muffling measured by calcium iontophoresis in snail neurones. *J Physiol.* **491**, (Pt 3), 621-633 (1996).
26. Chesler, M., Kraig, R. P. Intracellular pH of astrocytes increases rapidly with cortical stimulation). *Am J Physiol.* **253**, R666-R670 (1987).
27. Ammann, D., Chao, P. S., Simon, W. Valinomycin-based K+ selective microelectrodes with low electrical membrane resistance. *Neurosci Lett.* **74**, 221-226 (1987).
28. Deitmer, J. W. Bicarbonate-dependent changes of intracellular sodium and pH in identified leech glial cells. *Pflugers Arch.* **420**, 584-589 (1992).
29. Lux, H. D. Fast recording ion specific microelectrodes: their use in pharmacological studies in the CNS. *Neuropharmacology.* **13**, 509-517 (1974).
30. Nicholson, C., Phillips, J. M. Ion diffusion modified by tortuosity and volume fraction in the extracellular microenvironment of the rat cerebellum. *J Physiol.* **321**, 225-257 (1981).
31. Chesler, M., Chan, C. Y. Stimulus-induced extracellular pH transients in the in vitro turtle cerebellum. *Neuroscience.* **27**, 941-948 (1988).

32. Thomas, R. C. Intracellular sodium activity and the sodium pump in snail neurones. *J Physiol.* **220**, 55-71 (1972).